Spectrochimica Acta Part A: Molecular and Biomolecular Spectroscopy 188 (2018) 183–188

Contents lists available at ScienceDirect

Spectrochimica Acta Part A: Molecular and Biomolecular Spectroscopy

journal homepage: www.elsevier.com/locate/saa

Synthesis, physicochemical and optical properties of bis-thiosemicarbazone functionalized graphene oxide

Santosh Kumar [a,*], Mohmmad Y. Wani [a,1], Claudia T. Arranja [a], Ricardo A.E. Castro [b], José A. Paixão [c], Abilio J.F.N. Sobral [a,*]

[a] Department of Chemistry, University of Coimbra, P-3004-535 Coimbra, Portugal
[b] CEF, Faculty of Pharmacy, University of Coimbra, P-3000-548 Coimbra, Portugal
[c] Department of Physics, University of Coimbra, P-3004-516 Coimbra, Portugal

ARTICLE INFO

Article history:
Received 7 November 2016
Received in revised form 13 June 2017
Accepted 30 June 2017
Available online 1 July 2017

Keywords:
Graphene oxide
Bis-thiosemicarbazone
Characterization
Photoluminescence

ABSTRACT

Fluorescent materials are important for low-cost opto-electronic and biomedical sensor devices. In this study we present the synthesis and characterization of graphene modified with bis-thiosemicarbazone (BTS). This new material was characterized using Fourier transform infrared spectroscopy (FT-IR), Ultraviolet–visible (UV–Vis) and Raman spectroscopy techniques. Further evaluation by X-ray diffraction (XRD), thermo-gravimetric analysis (TGA), differential scanning calorimetry (DSC), scanning electron microscopy (SEM) and atomic-force microscopy (AFM) allowed us to fully characterize the morphology of the fabricated material. The average height of the BTSGO sheet is around 10 nm. Optical properties of BTSGO evaluated by photoluminescence (PL) spectroscopy showed red shift at different excitation wavelength compared to graphene oxide or bisthiosemicarbazide alone. These results strongly suggest that BTSGO material could find potential applications in graphene based optoelectronic devices.

1. Introduction

In recent decades, graphene oxide has taken on an assortment of diverse roles, not only in optoelectronics but also as a material for nanoscale engineering. Graphene oxide, as a graphene-based inorganic carbon material, possesses many exceptional properties including nanoscale controllability and biocompatibility which merit attention for many potential applications. As a robust yet flexible material it provides many possibilities for facile modification and fabrication to produce other desired graphene based materials [1–7]. Recently, graphene has advanced its applications in biomedical and energy engineering [8–10]. Also the improvement of graphene based fluorescent sensors for evaluating biomolecules has received great attention due to in situ cellular imaging studies [11]. In a recent study of chitosan/graphene oxide nanocomposite, it was found that the pH conditions affect the interaction between polymer and graphene oxide and hence the optical properties of the material [12]. Since graphene is a zero-bandgap semiconductor the possibility of observing luminescence is highly unlikely [13], and therefore, studies being conducted to increasing the band gap are important. An important strategy is to combine graphene oxide with some conjugated organic molecule to improve its optical properties.

Thiosemicarbazones constitute an interesting class of compounds with wide pharmacological versatility with anti-tumor, anti-cancer, anti-inflammatory, anti-protozoal, anti-bacterial and anti-viral activities [14–19]. Due to the presence of a conjugated system of double bonds and heteroatoms in the bis-thiosemicarbazone skeleton, it was speculated that the conjugation or fabrication of bis-thiosemicarbazone with graphene oxide could enhance the optical properties of graphene oxide. Despite the large amount of work done on graphene oxide, no literature precedents were found describing the fabrication and the study of the optical properties of bis-thiosemicarbazone-graphene oxide materials. We herein report the synthesis, physico-chemical and optical properties of BTSGO, a new material with potential to be applied as optical sensor or biosensor.

2. Experimental Section

2.1. Materials and Reagents

Graphite, 30% H_2O_2, $KMnO_4$, benzene-1,4-dicarbaldehyde and thiosemicarbazide were purchased from Sigma-Aldrich Co., (USA).

* Corresponding authors.
E-mail addresses: santoshics@gmail.com, santosh.kumar@uc.pt (S. Kumar), asobral@ci.uc.pt (A.J.F.N. Sobral).
[1] Present address: Texas Therapeutics Institute, Brown Foundation Institute of Molecular Medicine, The University of Texas Health Science Center at Houston, 1881 East Road, Houston, 77,054, Texas, United States.

http://dx.doi.org/10.1016/j.saa.2017.06.045
1386-1425/

Hydrochloric acid, $SOCl_2$ and H_2SO_4 was obtained from Merck (Germany) and were used without further purification.

2.2. Synthesis of Bis-thiosemicarbazone (BTS) (*3*)

Bis-thiosemicarbazone (BTS) was synthesized as outlined in Scheme 1. Benzene-1,4-dicarbaldehyde (**1**) (1 mmol, 0.13 g) was mixed with thiosemicarbazide (**2**) (2 mmol, 0.18 g) in ethanol with few drops of 10% NaOH, and placed in reflux for 5 h. Completion of the reaction was monitored by thin layer chromatography (TLC). After completion of the reaction, a pale yellow precipitate of BTS (**3**) was formed, which was filtered, dried and recrystallized in dichloromethane.

Yield 85%; IR ν_{max} cm^{-1}: 3396 (NH), 3264, 3191 (NH_2), 3010 (C—H), 1589 (C═C), 1515 (C═N), 1279 (C—N), 1120 (C═S); ^1H NMR (DMSO-d_6) δ(ppm): 8.30 (2H, s, —NH), 8.00 (2H, s, —CH═N), 7.80 (s, 4H, Ar), 3.35 (s, 4H, NH_2); ^{13}C NMR (DMSO-d_6) δ(ppm): 177.91 (C═S), 141.55 (C═N), 135.30, 127.42; ESI-MS *m/z*: $[M^+ + 1]$ 281.25, corresponding to the expected Mol. Formula $C_{10}H_{12}N_6S_2$.

2.3. Synthesis of Graphene Oxide

Graphene oxide (GO) was prepared by previous reported method of the oxidation of graphite using a modified Hummers method [12,20]. Natural graphite (3 g) was taken in a 250 mL round bottom flask and added to cold concentrated sulfuric acid (69 mL), which was stirring in the ice-bath. Potassium permanganate (9 g) was poured in the round bottom flask under stirring in an ice-bath. After that time the mixture was stirred at 35 °C for 2 h, and then distilled water (150 mL) was added slowly for 15 min to the mixture and raised the temperature (100 °C) it for another 15 min. The mixture was added into the 400 mL of 30% H_2O_2 aqueous solution. Then, the product was filtered and washed with 10% aqueous hydrochloric acid solution and finally powder was washed with distilled water. The brownish yellow powder obtained was dried under reduced pressure for 24 h.

2.4. Fabrication of Graphene Oxide-Bisthiosemicarbazone (BTSGO) Material (*5*)

For the fabrication of BTSGO, initially the carboxylic acid groups of GO were acylated with $SOCl_2$ in a 100 mL round bottom flask, using 200 mg of graphene oxide in 1 mL of DMF in N_2 atmosphere, under reflux. Solvent was removed by distillation, the crude product was washed with THF, centrifused and dried under vacuum. The obtained acylated product (**4**) was further treated with BTS in DMF to afford the desired material. The BTSGO was prepared in the following way: 87 mg of GOCl (**4**) was dissolved into 10 mL of DMF and 87 mg of BTS

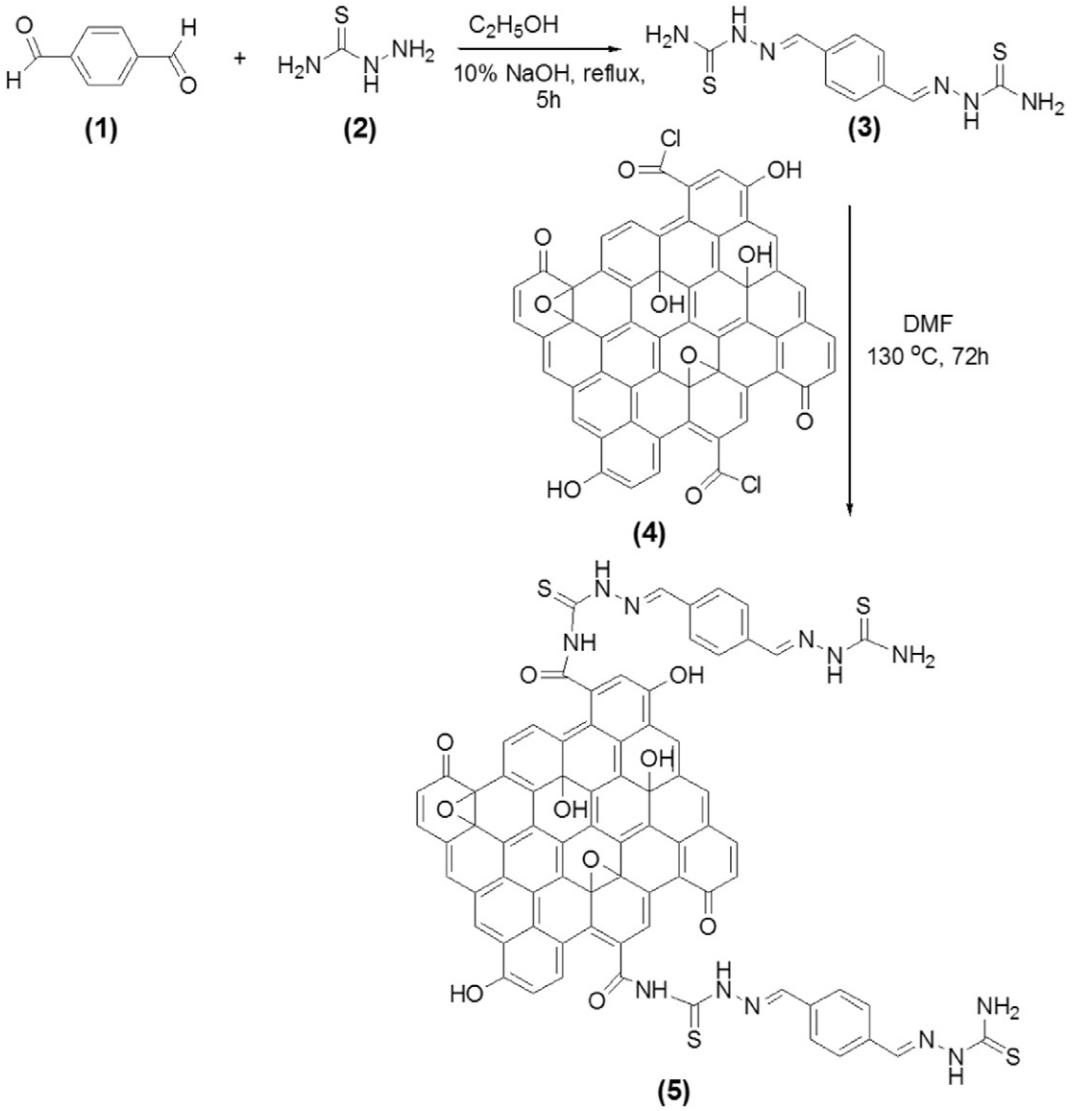

Scheme 1. Schematic illustration of the fabrication of BTSGO nanohybrid.

was allowed to react with the above solution at 130 °C for 72 h under an argon atmosphere. After the completion of the reaction, the solution was cooled to room temperature and the contents were poured into ethanol to precipitate the product. The product was obtained by filtration. The excess of BTS and other impurities were removed through washing with ethanol and the eluted was monitored by UV spectroscopy and TLC to ensure that no BTS existed in the final washing.

2.5. Characterization

Fourier transform infrared (FT-IR) spectra of the materials were recorded on a Thermo Nicolet IR300 FT-IR spectrometer with attenuated total reflectance (ATR) plate Smart Orbit Diamond, resolution 2 cm^{-1}, 64 scans. The Raman spectra were obtained by a Raman spectroscopy, Nicolet DXR Smart Raman, laser 514 nm (Ar-ion laser), power = 0.5 mW. The Powder X-ray diffraction (XRD) patterns were recorded using a Bruker D8 Advance diffractometer, equipped with a 3 kW generator, using Ni-filtered Cu Kα radiation (λ = 0.15418 nm) and a LYNXEYE detector. Data were collected in Bragg-Brentano geometry with a fixed 0.3° divergence slit. Thermogravimetry studies were performed in a Perkin-Elmer STA 6000 with a cooling unit providing a base temperature of 15 °C, and a dynamic nitrogen atmosphere flowing at 20 $mL \cdot min^{-1}$. Temperature calibration was performed with indium (Perkin-Elmer, x = 99.99%, T_{fus} = 156.60 °C) and zinc (Perkin-Elmer, x = 99.99%, T_{fus} = 419.53 °C). Samples were heated from 25 °C to 800 °C at rate of 20 °C min^{-1} in alumina crucibles. Scanning electron microscope (SEM) images were taken with a Tescan Vega3 SB scanning electron microscope. Images were collected using a secondary electron detector. AFM images were obtained at ambient conditions using a NTEGRA Prima NT-MDT instrument in semi contact mode. A NSG30 probe with a resonance frequency around 250 kHz was used. UV–visible absorption spectra were measured on an Agilent 8453 spectrophotometer (USA). ^{1}H NMR and ^{13}C NMR spectra were recorded on Bruker AVANCE 300 spectrometer using DMSO-d_6 as solvent with TMS as internal standard. Splitting patterns are designated as follows; s, singlet; d, doublet; dd, doublet of doublets; t, triplet; m, multiplet. Chemical shift values are given in ppm. ESI-MS was recorded on a Micromass Quattro II triple quadrupole mass spectrometer. Fluorescence spectra were obtained on a Horiba-Jobin-Yvon SPEX Fluorolog FL322.

3. Results and Discussion

3.1. Physico-chemical Characterization

Characteristic IR bands provide significant indications for the formation of BTS. The absence of a band at/or around 2665 cm^{-1} due to —C═O of benzene-1,4-dicarbaldehyde and the appearance of characteristic bands around at 1515 cm^{-1} region due to ν(C═N) stretch

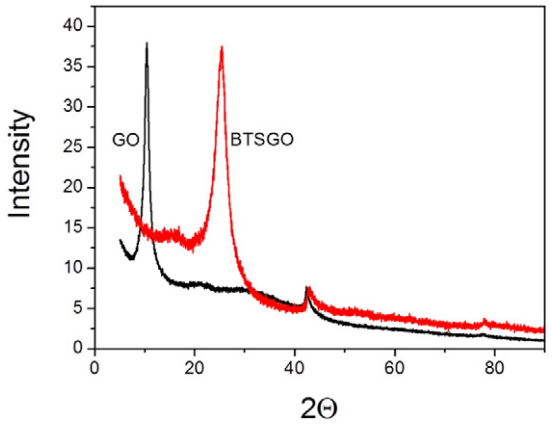

Fig. 2. XRD pattern of GO and BTSGO.

confirmed the formation of the BTS. Thiosemicarbazones may exhibit thione-thiol tautomerism, since they have a thione group (C═S) and proton adjacent to the thione group. It has been stated that the thione group (C═S) is relatively unstable in the monomeric form and tends to turn into a stable C—S single bond by tautomerism, if there is at least one hydrogen atom adjacent to the C═S bond. However, BTS showed intense, strong bands in the region 1081 and 805 cm^{-1} due to ν(C═S) stretch [21] and no band near 2570 cm^{-1} due to ν(C—SH), suggesting that this compound remains in the thione form. The FT-IR spectra of graphene oxide showed absorption band at 1724 cm^{-1}, characteristic of C═O stretching. The absorption peak at 1620 cm^{-1} is either assigned to the deformation of the OH band of the water absorbed by graphene oxide, or stretching of the aromatic C═C bond and 846 cm^{-1} to the characteristic absorption peak of epoxy groups. The FTIR spectra of BTSGO showed vibrational bands different from the corresponding materials, signifying some sort of interaction between GO and BTS as is evident from the distortion of amide bands of BTS in BTSGO.

Raman is supported to analyse changes in electronic structure due to C—C bonds and defects. Raman spectra of graphene oxide and BTSGO displayed two prominent peaks at about 1352 cm^{-1} (D band) and about 1590 cm^{-1} (G band), as shown in Fig. 1. However, the band intensity ratio ($r = I_D/I_G$) for BTSGO (r = 1.00) shows an enhanced value compared to that for graphene oxide (r = 0.84). BTSGO shows higher defect density compared to GO. The defects sites can be anticipated to play a positive role in contributing to the enhancement of photoluminescence.

X-ray diffractive region of pristine graphene oxide is observed at $2\theta = 11°$ [12]. Comparing the BTSGO diffractogram with that of GO we can see that the characteristic peak of GO is no longer present

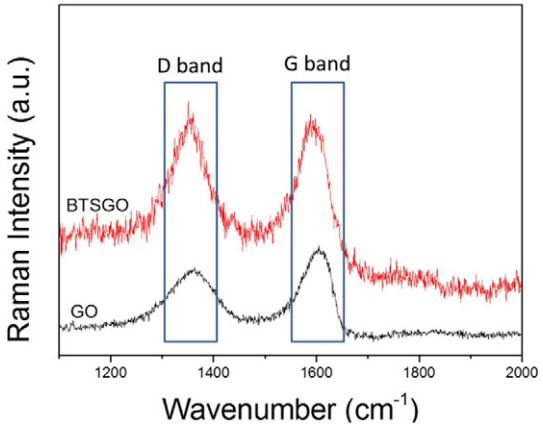

Fig. 1. Raman spectra of GO and BTSGO.

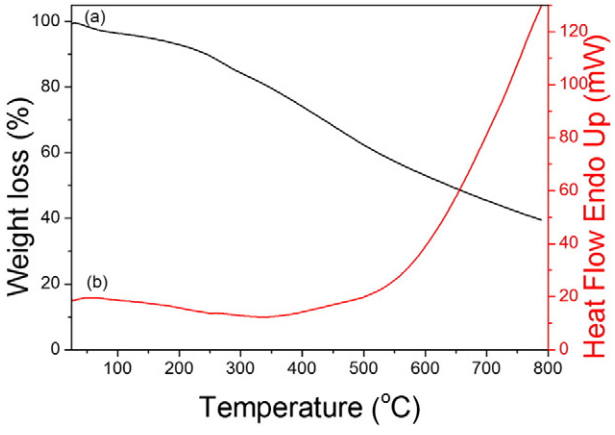

Fig. 3. TG/DSC curve of BTSGO.

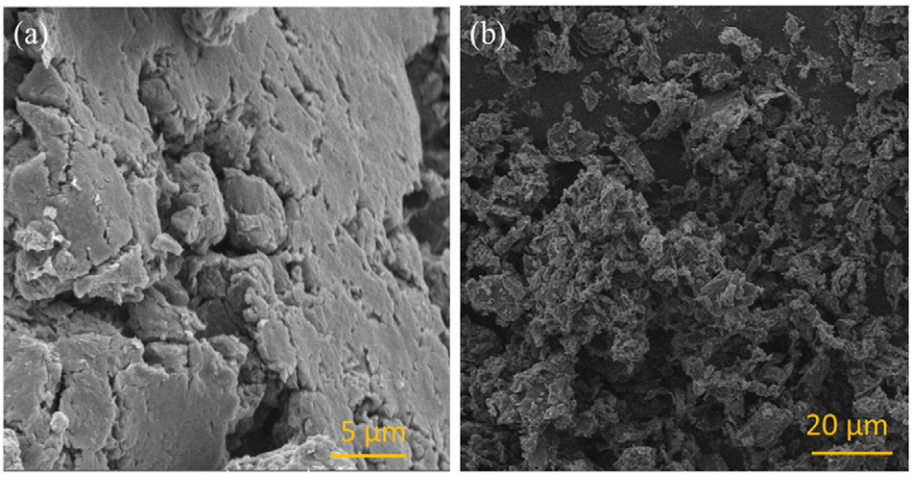

Fig. 4. SEM image of GO (a) and BTSGO (b).

and an intense peak is now found at a larger Bragg angle. The increase in *d*-spacing is due to the intercalation of amide functional groups in between graphene layers. BTSGO showed an intense sharp peak at around $2\theta = 25.45°$ and smaller peak at 42.79° (Fig. 2.). This shows the incorporation of BTS into the graphene oxide matrix.

3.2. Thermal Analysis

The thermal stability of the BTSGO was studied by thermogravimetric analysis as shown in Fig. 3a. The initial weight loss of BTSGO ca. 6% at around 45 °C, was due to evaporation of water, whereas the second stage of weight loss at 260 °C is due to the degradation of the BTS. In the corresponding DSC signal (Fig. 3b) it is only observable a small changes for the dehydration and another small endothermic event for the degradation. The mass loss of GO is ca. 7% at around 80 °C, which can be assigned to the removal of H_2O molecules adsorbed inside the GO structure (not shown in the Fig.3). A mass loss of ca. 55% occurring around 170 °C is ascribed to the pyrolysis of the labile oxygen-containing groups in the forms of CO, CO_2 and H_2O [22]. The change in the degradation temperature of BTSGO to a higher value shows that this material has higher thermal stability compared to GO.

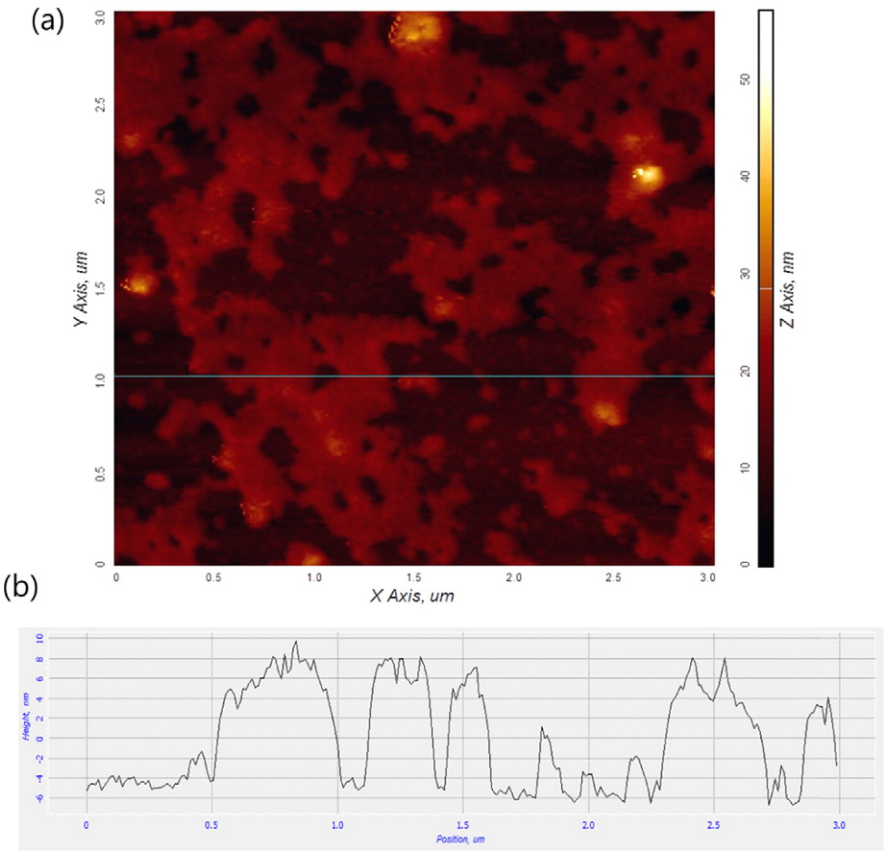

Fig. 5. (a) AFM image of BTSGO deposited on a glass substrate (a region of small coverage is shown to determine the thickness of the film). (b) Height profile of the film along the line depicted in a).

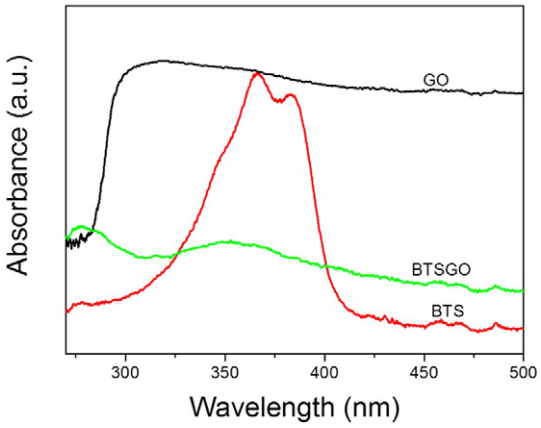

Fig. 6. UV–visible spectra of GO, BTS and BTSGO.

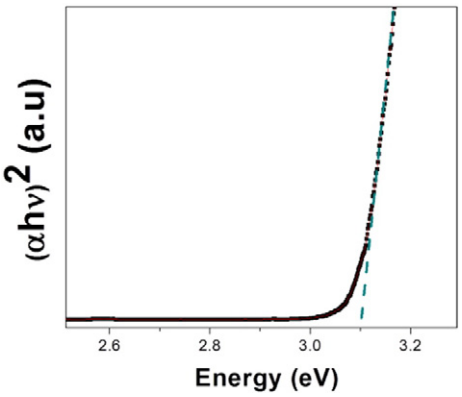

Fig. 7. Plot of $(\alpha h\nu)^2$ against Energy ($h\nu$) for BTSGO.

3.3. Surface Morphology

The morphology of the GO (Fig. 4a) and BTSGO (Fig. 4b) was investigated by scanning electron microscopy (SEM). The images of BTSGO showed a porous structure, confirming a strong effect of the BTS over the pristine GO. The AFM images shown in Fig. 5a and b indicate that BTSGO has an average thickness of around 10 nm indicating that BTSGO lies as a mixture of single and double-layered sheets. AFM image also reveals that the structure of BTSGO is formed as a result of the fabrication of BTS molecules on the GO surface, which gives an irregular texture to the BTSGO material, in the form of sheets.

3.4. UV–Vis Absorption Spectra

The UV–Vis spectra of graphene oxide, BTS and BTSGO in DMF solution are shown in Fig. 6. The graphene oxide has a characteristic shoulder around at 310–320 nm observed due to the n-π* transition of C═O [23]. BTS has two characteristic peaks at 366 and 383 nm. A characteristic absorption peak was observed in BTSGO at 360 nm due to π-π* transition. GO is unexplored in the field of optical application due to its poor optical property generated from zero band gap characteristics, however we observed that BTSGO has an optical energy band gap of 3.1 eV, a feature desirable for a graphene based material for use in optoelectronic devices [24] (Fig. 7).

3.5. Photoluminescence (PL) Study

The photoluminescence studies of graphene oxide and BTSGO were performed to understand its emission properties as shown in Fig. 8. The graphene oxide had emission spectrum (λ_{em}) peak at 320 nm at excitation wavelength of 278 nm (Fig. 8a). The PL spectrum of BTSGO showed emission maximum (λ_{em}) peak at 440 nm under excitation wavelength of 278 nm, which explains red-shifted emission maxima due to bandgap transitions corresponding to conjugated π-domains and the other with more complex origins that are more or less associated with defects in the graphene structure [25–26]. BTS itself did not show any photoluminescent properties but the presence of GO and BTS together in BTSGO resulted in photoluminescence, which could be due to the synergetic effect of chemical and physical properties of both BTS and GO. BTSGO is highly dispersible in DMF and emits light in the visible when stimulated with different excitation wavelengths. We have observed, the photoluminescence peak of the BTSGO at around 440 nm when the excitation wavelength changed from 278 nm to 320 nm (as shown in Fig. 8b), no PL peak shifting but a dramatic increase in photoluminescence intensity. The similar phenomenon is reported previously different from the general excitation dependent PL emissions, in which the PL peaks shift to longer wavelengths upon an increase in the excitation wavelengths [27–30]. Zhang et al. have reported opposite phenomenon, the intensity of the PL increased to the maximum then decreased on excited wavelengths ranging from 340 to 410 nm in the graphene quantum dots [31]. Xu et al. have also observed the photoluminescence of fabricated nitrogen-doped graphene quantum dot at different excitation wavelengths [32].

4. Conclusions

The fascinating properties of graphene oxide derivatives such as functionalizable surfaces, strong UV absorption and photoluminescence ability make them one of the most promising materials for biosensors. We fabricated a new graphene based material and characterized it

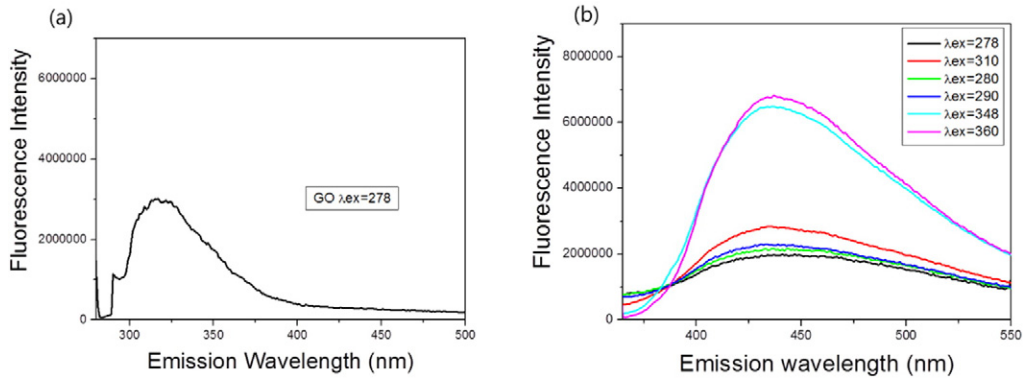

Fig. 8. (a) The fluorescence spectrum of GO were obtained at excitation wavelength 278 nm. (b) The fluorescence spectra of BTSGO were obtained at different excitation wavelengths ranging from 278 to 360 nm.

using UV–Vis, FT-IR, Raman and X-ray diffractometry analysis. The morphological study indicates surface of the fabricated material. The thermal studies showed that this material is thermally more stable than graphene oxide. The photoluminescence spectra showed optical properties. Our findings points to the possibility of BTSGO be used as a tool for biomedical applications, where a strong photoluminescent graphene based material can be used.

Acknowledgements

Thanks are due to the European Regional Development Fund-QREN-COMPETE for funding the project PTDC/AAC-CLI/118092/2010 coordinated by Prof. Abilio Sobral, and Centro de Quimica by PEst-C/QUI/UI0313/2014) and FCT, Portugal for his grant S. Kumar (SFRH/BPD/86507/2012), M.Y. Wani (SFRH/BPD/86581/2012) and Access to TAIL-UC facility funded under QREN-Mais Centro Project ICT/2009/02/012/1890 is gratefully acknowledged.

References

[1] Z. Gan, H. Xu, Y. Hao, Nano 8 (2016) 7794.
[2] X. Michalet, F.F. Pinaud, L.A. Bentolila, J.M. Tsay, S. Doose, J.J. Li, G. Sundaresan, A.M. Wu, S.S. Gambhir, S. Weiss, Science 307 (2005) 538.
[3] C. Chung, Y. Kim, D. Shin, S.R. Ryoo, B.H. Hong, D. Min, Acc. Chem. Res. 46 (2013) 2211.
[4] Y.L. Liu, X.Y. Wang, J.Q. Xu, C. Xiao, Y.H. Liu, X.W. Zhang, J.T. Liu, W.H. Huang, Chem. Sci. 6 (2015) 1853.
[5] (a) H. Jang, J. Lee, D.H. Min, J. Mater. Chem. B 2 (2014) 2452;
(b) J. Chatopadhyay, R. Srivastava, P.K. Srivastava, Int. J. Electrochem. Sci. 8 (2013) 3740.
[6] A. Ambrosi, C.K. Chua, N.M. Latiff, A.H. Loo, C.H.A. Wong, A.Y.S. Eng, A. Bonanni, M. Pumera, Chem. Soc. Rev. 45 (2016) 2458–2493.
[7] C.V. Pham, M. Krueger, M. Eck, S. Weber, E. Erdem, Appl. Phys. Lett. 104 (2014) 132102.
[8] (a) X. Zou, L. Zhang, Z. Wang, Y. Luo, J. Am. Chem. Soc. 138 (2016) 2064;
(b) Y. Zhang, Q. Tang, B. He, P. Yang, J. Mater. Chem. A 4 (2016) 13235.
[9] S. Kumar, M.Y. Wani, J. Koh, J. Gil, A.J.F.N. Sobral, J. Environ. Sci. (2017) http://dx.doi.org/10.1016/j.jes.2017.04.013.
[10] P.K. Dutta, R. Srivastava, J. Dutta, Adv. Polym. Sci. 254 (2013) 1.
[11] L. Zhang, S.J. Xiao, L.L. Zheng, Y.F. Li, C.Z. Huang, J. Mater. Chem. B 2 (2014) 8558.
[12] S. Kumar, J. Koh, Int. J. Biol. Macromol. 70 (2014) 559.
[13] G. Eda, Y. Lin, C. Mattevi, H. Yamaguchi, H.A. Chen, I. Chen, C.W. Chen, M. Chhowalla, Adv. Mater. 22 (2010) 505.
[14] H. Beraldo, D. Gambino, Mini-Rev. Med. Chem. 4 (2004) 31.
[15] D. Palanimuthu, S.V. Shinde, K. Somasundaram, A.G. Samuelson, J. Med. Chem. 56 (2013) 722.
[16] B. Ma, B.C. Goh, E.H. Tan, K.C. Lam, R. Soo, S.S. Leong, L.Z. Wang, F. Mo, A.T.C. Chan, B. Zee, T. Mok, Investig. New Drugs 26 (2008) 169.
[17] H.B. Shawish, W.Y. Wong, Y.L. Wong, S.W. Loh, C.Y. Looi, P. Hassandarvish, A.Y. Phan, W.F. Wong, H. Wang, I.C. Paterson, C.K. Ea, M.R. Mustafa, M.J. Maah, PLoS One 9 (2014), e100933.
[18] R.A. Finch, M.C. Liu, A.H. Cory, J.G. Cory, A.C. Sartorelli, Adv. Enzym. Regul. 39 (1999) 3.
[19] W. Antholine, J. Knight, H. Whelan, D.H. Petering, Mol. Pharmacol. 13 (1977) 89.
[20] (a) W.S. Hummers, R.E. Offeman, J. Am. Chem. Soc. 80 (1958) 1339;
(b) C. Hou, Q. Zhang, M. Zhu, Y. Li, H. Wang, Carbon 49 (2011) 47.
[21] D.M. Wiles, B.A. Gingkas, F. Suprlnch, Can. J. Chem. 45 (1907) 469.
[22] J. Shen, Y. Hu, M. Shi, X. Lu, C. Qin, C. Li, M. Ye, Chem. Mater. 21 (2009) 3514.
[23] Z. Luo, Y. Lu, L.A. Somers, A.T.C. Johnson, J. Am. Chem. Soc. 131 (2009) 898.
[24] Y. Shen, S. Yang, P. Zhou, Q. Sun, P. Wang, L. Wan, J. Li, L. Chen, X. Wang, S. Ding, D.W. Zhang, Carbon 62 (2013) 157.
[25] L. Cao, M.J. Meziani, S. Sahu, Y.P. Sun, Acc. Chem. Res. 46 (2013) 171.
[26] C.V. Pham, S. Repp, R. Thomann, M. Krueger, S. Weberc, E. Erdem, Nano 8 (2016) 9682.
[27] S.K. Cushing, M. Li, F. Huang, N. Wu, ACS Nano 8 (2014) 1002.
[28] Q. Mei, K. Zhang, G. Guan, B. Liu, S. Wang, Z. Zhang, Chem. Commun. 46 (2010) 7319.
[29] S. Kumar, P. Garg, S. Pandey, M. Kumari, S. Hoon, R. Kapavarapu, P.H. Choung, A.J.F.N. Sobral, J.H. Chung, J. Mater. Chem. B 3 (2015) 3465.
[30] P.C. Hsu, P. Chen, C.M. Ou, H.Y. Chang, H.T. Chang, J. Mater. Chem. B 1 (2013) 1774.
[31] M. Zhang, L. Bai, W. Shang, W. Xie, H. Ma, Y. Fu, D. Fang, H. Sun, L. Fan, M. Han, C. Liu, S. Yang, J. Mater. Chem. 22 (2012) 7461.
[32] H. Xu, S. Zhou, L. Xiao, H. Wang, S. Li, Q. Yuan, J. Mater. Chem. C 3 (2015) 291.